XLVI CILAMCE
VITÓRIA - ES - BRAZIL - 2025
XLVI IBERO-LATIN AMERICAN CONGRESS ON COMPUTATIONAL METHODS IN ENGENEERING

Optimal Tower Sizing of the IEA-15MW Offshore Wind Turbine Under Site-Specific Loading

Gino B. Colherinhas[1], Hisham Tariq[2], Marcus V. G. Morais[3], Francesco Petrini[4], Agathoklis Giaralis[2]

[1]*Escola de Engenharia Elétrica, Mecânica e de Computação, Universidade Federal de Goiás*
Alameda Ingá, Prédio B5, Campus Samambaia, 74045-155. Goiânia, Goiás, Brazil
gino@ufg.br
[2]*Department of Civil and Environmental Engineering, Khalifa University of Science and Technology*
Abu Dhabi, 127788, United Arab Emirates
{100063744,agathoklis.giaralis}@ku.ac.ae
[3]*Faculdade de Tecnologia, Universidade de Brasília*
Campus Darcy Ribeiro, Asa Norte, 70910-900. Brasília, Distrito Federal, Brazil
mvmorais@unb.br
[4]*Facoltà di Ingegneria, Sapienza Università di Roma*
Dipartimento di Ingegneria Strutturale e Geotecnica, Via Eudossiana 18, Roma, 00184, Italy
francesco.petrini@uniroma1.it

Abstract. This study presents the optimal structural redesign of the IEA-15MW offshore wind turbine tower using a single-objective genetic algorithm coupled with a high-fidelity finite element model implemented in PyMAPDL. The optimization aims to minimize the tower mass while satisfying stress, frequency, displacement, geometric, and buckling constraints under site-specific environmental conditions. Four representative Design Load Cases (DLCs) were considered—normal, extreme, and idling sea states—based on wind and wave spectra typical of Northern Europe. Spectral dynamic responses were computed via power spectral density (PSD) analysis and applied in combination with static wind and wave loading. All optimizations converged to a single robust structural configuration, leading to a 9.94% mass reduction compared to the IEA-15MW reference design and a reduction in first natural frequency from 0.173 Hz to 0.140 Hz, satisfying the dynamic regime. Post-optimization buckling verification was performed based on Eurocode 3 Part 1–6, confirming shell stability under combined axial and shear stresses. The proposed framework demonstrates the potential of customized GA-based workflows for efficient and constraint-aware offshore tower design.

Keywords: Optimal Sizing, Genetic Optimization, Offshore Wind Turbine, Structural Dynamics, Power Spectral Density.

1 Introduction

The design of support structures for next-generation offshore wind turbines (OWTs) presents significant engineering and economic challenges, especially for turbines exceeding 10 MW in capacity. As part of global efforts to decarbonize power generation, the IEA-15MW Reference Wind Turbine (RWT) developed by NREL [1] has been recently proposed as a benchmark OWT to facilitate design and analysis of large-scale OWTs. This reference turbine features a hub height of 150 m and a 240 m rotor diameter, supported by a monopile-tower structure.

Recent studies in the field of offshore wind turbine support structures have emphasized the need for integrated design approaches that combine structural optimization, manufacturing feasibility, and advanced control strategies. Comprehensive reviews have highlighted trends in tower design, including the adoption of soft–stiff configurations, the importance of diameter-to-thickness constraints, and the potential of AI-driven frameworks for future design automation [2]. Additionally, successful applications of finite element modeling combined with genetic algorithms have demonstrated substantial gains in structural efficiency and material reduction [3]. These efforts collectively motivate the development of customized optimization workflows capable of incorporating site-specific loading, modern simulation tools, and tailored constraint formulations.

While various tools such as Wind-Plant Integrated System Design and Engineering Model (WISDEM) have been used for the optimal sizing of support structure of OWTs based on a static linear elastic finite element analysis

[4], this paper introduces an alternative approach based on an in-house implementation using PyMAPDL coupled with a genetic algorithm (GA) coded in Python. The work builds upon previous modeling efforts of the 15 MW tower developed by Colherinhas et al. [5, 6], where a FE model with fixed-base boundary conditions at the mudline was created using ANSYS® Mechanical APDL. Herein, improvements are implemented in the structural modeling and load estimation routines, enabling a more accurate and site-specific dynamic response evaluation. Further, a Single-Objective Optimization (SOO) problem is formulated to minimize the structural mass of the support tower, while ensuring compliance with frequency, stress, buckling, and displacement criteria under site-specific loading.

2 Modeling and Environmental Conditions

2.1 Benchmark OWT description and modeling

The IEA-15MW-RWT consists of a 3-bladed upwind rotor mounted on a monopile foundation. The tower transitions from an outer diameter of 10 m at the base to 6.5 m at the nacelle interface, with a total height of approximately 174.4 m, including 45 m embedded and 30 m submerged monopile sections. In this study, redesign efforts focus on the structural tower and monopile dimensions (diameter and thickness), starting from the benchmark profile provided by NREL [1]. Figure 1 illustrates the OWT structural configuration and the main environmental loading applied in the simulations.

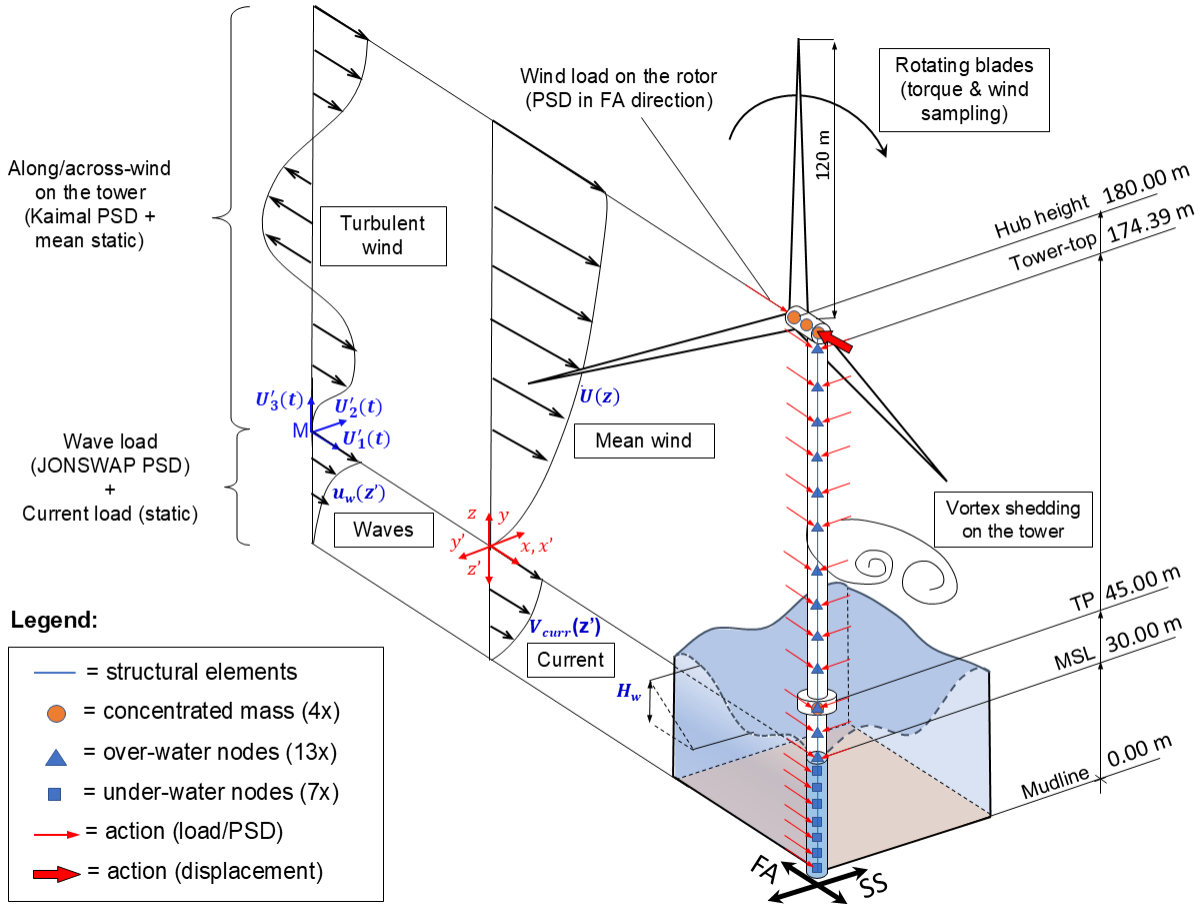


Figure 1. Schematic representation of loads on the IEA-15MW OWT.

The structural model comprises 13 over-water and 7 submerged nodes connected by BEAM188 elements, representing the flexible tower and monopile, which is assumed to be rigidly connected at the mudline. Four additional MASS21 elements are included to simulate the rotor-nacelle assembly and transition piece masses. All simulations are performed in the frequency domain using spectral analysis, where wind and wave excitations are

decomposed into power spectral densities (PSDs) applied at each node. The dynamic response is computed from the resulting nodal displacements, while static analyses account for mean wind and wave loading.

2.2 Wind Field and Wind-Induced Loads

Wind excitation is modeled based on the Kaimal turbulence spectrum and IEC 61400-1 standards. Aerodynamic loads on the rotor are computed using a Blade Element Momentum (BEM) model implemented in Python, following the AeroDyn manual [7] and Burton et al. [8]. The model incorporates tabulated airfoil data and accounts for blade pitch, twist, tip and hub losses, and the Glauert correction. For a given wind speed at hub height, the pitch angle and rotational speed are interpolated from turbine control tables. The axial and tangential induction factors are iteratively calculated at each blade section to determine the distributed forces. The resulting thrust and torque are transferred to the finite element model as external loads.

The wind field is discretized along the tower height, and site-specific wind spectra are computed for the along-, across-, and upwind components. The resulting PSDs, including rotationally sampled contributions, are used in the frequency-domain analysis to evaluate structural response.

2.3 Wave and Sea Current Dynamics

Sea currents in shallow waters are modeled by a velocity profile that decays with depth. Following DNV-OS-J101 [9], the total current velocity $V_{\text{curr}}(z')$ at a given depth z' is expressed as:

$$V_{\text{curr}}(z') = v_{\text{tide}}(z') + v_{\text{wind}}(z'), \tag{1}$$

$$v_{\text{tide}}(z') = v_{\text{tide0}} \left(\frac{h_0 - z'}{h_0} \right)^{1/7}, \quad v_{\text{wind}}(z') = v_{\text{wind0}} \left(\frac{h_0 - z'}{h_0} \right), \quad \text{for } -h_0 \leq z' \leq 0$$

where v_{tide0} and v_{wind0} are the surface tidal and wind-induced current velocities at still water level (SWL), and h_0 is the reference depth, typically 50 m. The wind-generated current is computed as $v_{\text{wind0}} = k \cdot V_{10-1h}$, with k ranging from 0.015 to 0.03 and V_{10-1h} representing the 1-hour averaged wind speed at 10 m height.

Hydrodynamic excitation is modeled using linear wave theory, with particle velocities and accelerations estimated at each submerged node based on the JONSWAP spectrum. The wave-induced drag and inertia forces per unit length at a depth z' are calculated using the linearized Morison equation:

$$F_{I+D}(x, z', t) = C_I H_w(\omega, z') \ddot{\eta}(x, t) + C_D \sqrt{\frac{8}{\pi}} \sigma_u \left[H_w(\omega, z') \dot{\eta}(x, t) + V_{\text{curr}}(z') \right] \tag{2}$$

Here, $H_w(\omega, z')$ is the wave transfer function at depth z', $\eta(x, t)$ is the sea surface elevation, and $V_{\text{curr}}(z')$ is the local current velocity. σ_u denotes the standard deviation of wave-induced horizontal velocity, and C_D, C_I are the drag and inertia coefficients, respectively.

Assuming $\eta(x, t)$ is a stationary stochastic process, the associated wave force spectrum $S_F(x, z', \omega)$ is given by:

$$S_F(x, z', \omega) = \left(C_I^2 \omega^4 + \frac{8}{\pi} \sigma_u^2 C_D^2 \omega^2 \right) H_w^2(\omega, z') S_{JS}(x, \omega) \tag{3}$$

where S_{JS} is the JONSWAP sea-surface elevation spectrum computed from the parameters listed in Table 1. The resulting force spectra are calculated at each submerged node and superimposed with wind and rotor-induced spectra to evaluate the full structural response.

Table 1. Environmental parameters used in the optimization for each DLC

DLC	Turbine Class	Wind velocity at hub height [m/s]	Wave conditions
1.2	C	10.59	H_s = 0.75 m; T_p = 10.5 s; γ = 1.000
1.6	C	10.59	H_s = 9.25 m; T_p = 15.789 s; γ = 1.708
6.1.1	B	29.63	H_s = 5.93 m; T_p = 13.024 s; γ = 1.394
6.1.2	B	40.55	H_s = 9.25 m; T_p = 15.789 s; γ = 1.708

2.4 Dynamic Structural Response

The computed PSDs are used to estimate the standard deviation of the displacement response (σ_r), which is combined with the mean static displacement (r_m) to obtain the peak response:

$$r_p = r_m + g_r \cdot \sigma_r \tag{4}$$

where g_r is a response peak factor given by:

$$g_r = \sqrt{2\ln(n_1 \cdot T_{wind})} + \frac{0.577}{\sqrt{2\ln(n_1 \cdot T_{wind})}}, \quad T_{wind} = 3600 \text{ s} \tag{5}$$

In the across-wind direction, vortex-induced vibrations are considered using the semi-empirical formulation from [9, 10]:

$$r_{VS}^{across} = \frac{1.29D}{1 + 0.43(2\pi ScSt^2)}, \quad \text{for } \frac{0.8}{St} \leq U_R \leq \frac{1.6}{St} \tag{6}$$

where $U_R = U_{hub}/(n_1 D)$, and Sc and St are the Scruton and Strouhal numbers, respectively.

The peak displacement r_p is subsequently applied as a static load at the tower top to compute resultant stresses for design verification.

3 Optimization Framework and Redesign Constraints

To guide the optimization process, a set of eleven constraints was formulated based on DNV standards and recent literature [4]. These include: maintaining a minimum diameter-to-thickness ratio of 80 and a region-dependent upper bound of 260 for the monopile and 300 for the tower section, adopted as preliminary buckling design limits; ensuring the first natural frequency exceeds 0.14 Hz to avoid resonance with 1P excitations; limiting base stresses to remain below the material yield strength divided by appropriate partial safety factors; enforcing geometric monotonicity, with non-increasing diameter and wall thickness profiles; bounding the diameters between 6.0 m and 12.0 m and the thicknesses between 4 mm and 100 mm; and constraining hub displacement under environmental loading to a maximum of 2% of the total tower height [2].

These constraints were incorporated via a penalty-based formulation in the optimization problem, implemented using the `pymoo` Python library [11]. The algorithm applies standard genetic operators—selection, SBX crossover, and polynomial mutation—and evaluates each candidate solution through a fully coupled finite element model written in PyMAPDL, allowing for automated and constraint-aware structural assessments.

A final buckling check was performed for the optimal solutions to assess the shell stability under combined axial and shear stresses. The implementation follows the approach proposed in Zhang et al. [12], where local shell buckling utilization is evaluated at each conical section using the Eurocode 3 Part 1–6 formulation. Circumferential stresses were conservatively assumed to be zero, as axial and shear components dominate the loading regime under power production and idling conditions.

$$Y_{\text{ULS},2} = \left(\frac{\sigma}{\sigma_{x,Rd}}\right)^{k_x} + \left(\frac{\tau}{\tau_{x\theta,Rd}}\right)^{k_\tau} \leq 1 \tag{7}$$

In this expression, σ is the meridional (axial) stress and τ is the shear stress, both extracted from the PyMAPDL solution and averaged over each shell segment. The design buckling resistances $\sigma_{x,Rd}$ and $\tau_{x\theta,Rd}$ are computed based on the Eurocode reduction factors, which consider the shell geometry, taper ratio, material yield strength, and fabrication quality. Spline-based smoothing functions were applied to ensure continuity in the stiffness and interaction terms. The exponents k_x and k_τ represent interaction parameters that depend on the reduction factors and are defined in the standard. This criterion was applied to all tapered shell sections of the optimal design, enabling a conservative buckling verification.

4 Results and Discussion

To evaluate the structural performance of the IEA-15MW offshore wind turbine tower under different environmental conditions, four independent optimizations were carried out, each corresponding to a specific Design

Load Case (DLC): 1.2, 1.6, 6.1.1, and 6.1.2. All cases were optimized using a single-objective genetic algorithm (SOO) configured to minimize structural mass under the constraints described in Section 3. The algorithm employed a population size of 100 individuals over 150 generations, using standard simulated binary crossover (SBX) with 90% crossover probability and distribution index $\eta = 15$, along with polynomial mutation with $\eta = 20$. To maintain diversity and avoid premature convergence, identical individuals were excluded from the population at each generation.

Despite the distinct environmental loads across the four DLCs, the optimizer consistently converged to the same structural configuration. Figure 2 illustrates the optimized outer diameter and wall thickness distributions, compared to the IEA-15MW-RWT reference model. The optimized solution presents significant reductions in upper tower diameters and a more uniform thickness profile, contributing to improved material efficiency.

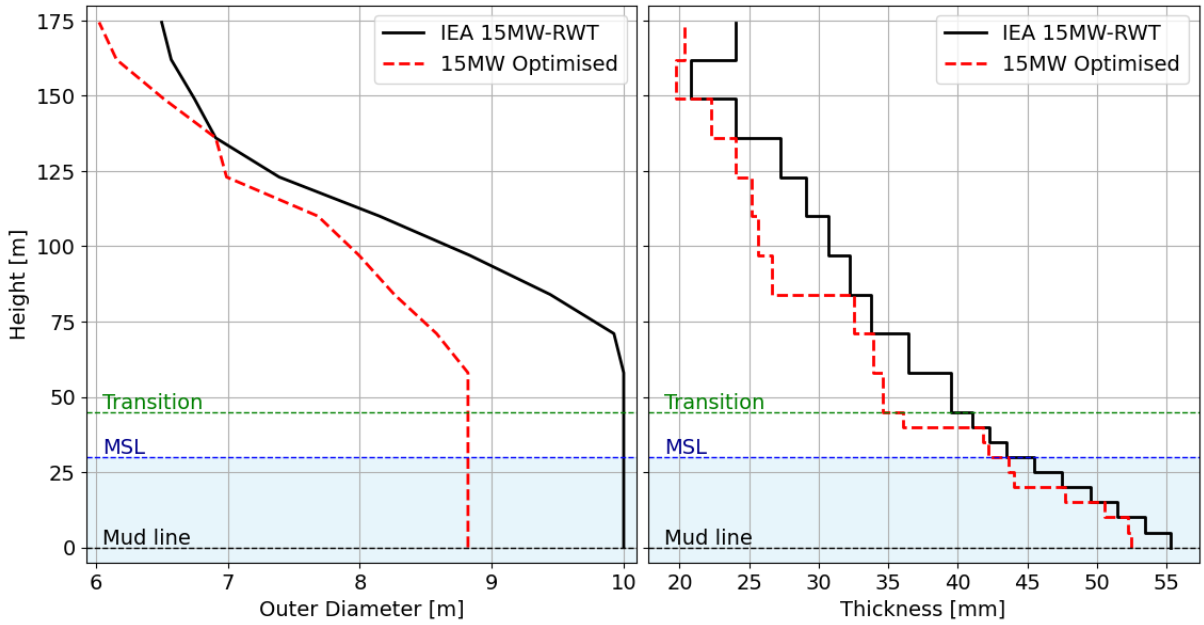


Figure 2. Comparison between the optimized tower design and the IEA-15MW-RWT in terms of outer diameter and wall thickness distributions.

The optimized configuration reduced the structural mass from $2368.00\,\mathrm{t}$ (IEA-15MW-RWT) to $2132.62\,\mathrm{t}$, representing a decrease of **9.94%**. Additionally, the first natural frequency decreased from $0.173\,\mathrm{Hz}$ to $0.140\,\mathrm{Hz}$, reaching the lower bound imposed to prevent resonance with 1P rotor excitation.

Table 2. Dynamic response and stress results for each DLC using the optimized tower

DLC	Max. Stress [MPa]	Disp. (Along) [m]	Disp. (Across) [m]	Result. Hub Displacement [m]
1.2	122.89	1.26	0.41	1.33
1.6	154.47	1.52	0.72	1.69
6.1.1	161.14	1.56	0.81	1.76
6.1.2	192.78	1.85	1.10	2.15

All results comply with the displacement constraint of 2% of the total tower height and the stress constraint of $196.7\,\mathrm{MPa}$, derived from the material yield strength of $345\,\mathrm{MPa}$ divided by the partial safety factors 1.35 and 1.3. Even under the extreme combined wind and wave conditions of DLC 6.1.2, the structural integrity is maintained without exceeding stress or displacement limits. This confirms the adequacy of the optimized configurations in satisfying ultimate limit state requirements for all design load cases.

Figure 3 shows the shell buckling utilization $Y_{\mathrm{ULS},2}$ computed along the tower elevation for each DLC, following the Eurocode 3 Part 1–6 methodology. All sections remained below the critical threshold ($Y_{\mathrm{ULS},2} \leq 1$), confirming that the final design preserves structural stability under all evaluated site-specific conditions.

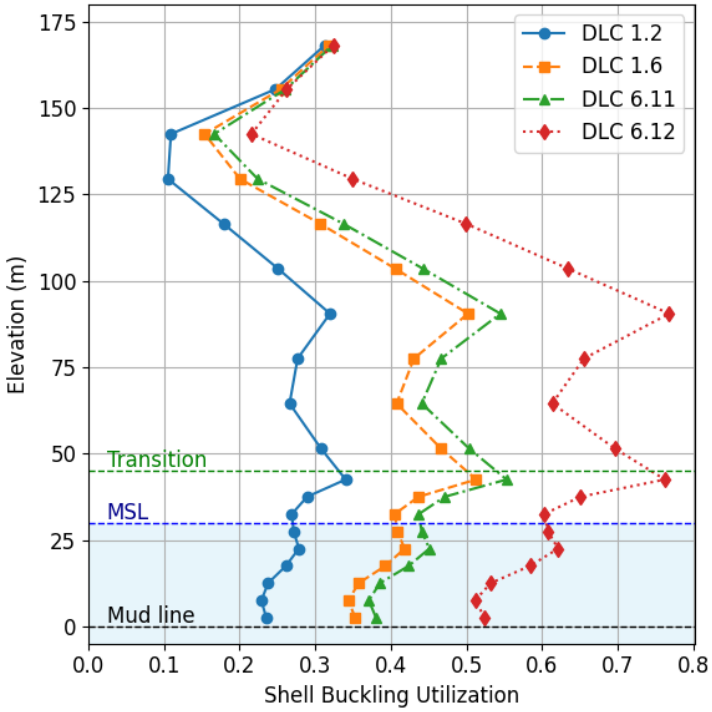


Figure 3. Shell buckling utilization for the optimized tower across all DLCs.

5 Conclusions

This work presented a structural optimization framework for the IEA-15MW offshore wind turbine tower using a single-objective genetic algorithm coupled with a fully parametric finite element model in PyMAPDL. The methodology allowed the integration of site-specific environmental loading—derived from four representative Design Load Cases (DLCs)—into a constraint-aware mass minimization process.

The results demonstrated that, despite the varying loading conditions across all DLCs, the optimizer consistently converged to a single robust design. Compared to the IEA-15MW reference configuration, the optimized solution achieved a mass reduction of around 10%, while maintaining compliance with displacement, stress, and frequency constraints. The first natural frequency was reduced to 0.140 Hz, ensuring dynamic compatibility with 1P rotor excitations.

A post-optimization verification of local shell stability was performed using the Eurocode 3 Part 1–6 formulation. The calculated buckling utilization factors remained below the critical limit across all tapered sections of the optimized design, even under extreme load cases, validating the structural feasibility of the proposed layout. The developed framework offers a flexible and efficient alternative to traditional design tools, enabling rapid exploration of design spaces while preserving compliance with regulatory criteria.

Acknowledgements. The authors acknowledge the financial support provided by FAPEG (Fundação de Amparo à Pesquisa do Estado de Goiás) and CNPq (Conselho Nacional de Desenvolvimento Científico e Tecnológico), which made this research possible.

Authorship statement. The authors hereby confirm that they are the sole liable persons responsible for the authorship of this work, and that all material that has been herein included as part of the present paper is either the property (and authorship) of the authors, or has the permission of the owners to be included here.

References

[1] E. Gaertner, J. Rinker, L. Sethuraman, F. Zahle, B. Anderson, G. Barter, N. Abbas, F. Meng, P. Bortolotti, W. Skrzypinski, G. Scott, R. Feil, H. Bredmose, K. Dykes, M. Sheilds, C. Allen, and A. Viselli. Definition of the IEA 15-megawatt offshore reference wind turbine. Technical report, Technical University of Denmark, International Energy Agency, 2020.

[2] J. Alves Ribeiro, B. Alves Ribeiro, F. Pimenta, S. M.O. Tavares, J. Zhang, and F. Ahmed. Offshore wind turbine tower design and optimization: A review and ai-driven future directions. *Applied Energy*, vol. 397, pp. 126294, 2025.
[3] T. Gentils, L. Wang, and A. Kolios. Integrated structural optimisation of offshore wind turbine support structures based on finite element analysis and genetic algorithm. *Applied Energy*, vol. 199, pp. 187–204, 2017.
[4] H. Tariq, G. Mylonakis, M. Al-Shudaifat, J.-C. Gilloteaux, and A. Giaralis. Integrated sizing and vibration control of monopile iea-15mw benchmark offshore wind turbine. In *Proceedings of the 10th ECCOMAS Thematic Conference on Computational Methods in Structural Dynamics and Earthquake Engineering (COMPDYN 2025)*, pp. 1–18, Rhodes Island, Greece. ECCOMAS, 2025.
[5] G. B. Colherinhas, F. Petrini, de M. V. G. Morais, and F. Bontempi. Optimal design of passive-adaptive pendulum tuned mass damper for the global vibration control of offshore wind turbines. *Wind Energy*, vol. 24, n. 6, pp. 573–595, 2021.
[6] G. B. Colherinhas, M. V. G. Morais, M. R. Machado, and F. Petrini. Modeling and dynamic analysis of 15 and 22-megawatt offshore wind turbines using pymapdl. In *Proceedings of the XLV Ibero-Latin-American Congress on Computational Methods in Engineering (CILAMCE 2024)*, Maceió, Alagoas, Brazil. ABMEC, 2024.
[7] P. J. Moriarty and A. C. Hansen. Aerodyn theory manual. Technical report, National Renewable Energy Laboratory, NREL/TP-500-36881, 2005.
[8] N. Jenkins, T. Burton, E. Bossanyi, D. Sharpe, and M. Graham. *Wind Energy Handbook 3e*. Wiley, 2021.
[9] DNVGL. *Recommended practice: environmental conditions and environmental loads*. DNV-GL-RP-C205 Standard, 2017.
[10] C. Borri and S. Pastò. *Lezioni di ingegneria del vento*, volume 1. Firenze university press, 20 edition, 2006.
[11] J. Blank and K. Deb. pymoo: Multi-objective optimization in python. *IEEE Access*, vol. 8, pp. 89497–89509, 2020.
[12] Z. Zhang, R. De Risi, and A. Sextos. Multi-hazard fragility assessment of monopile offshore wind turbines under earthquake, wind and wave loads. *Earthquake Engineering & Structural Dynamics*, vol. 52, n. 9, pp. 2658–2681, 2023.